Monthly Notices of the ROYAL ASTRONOMICAL SOCIETY

MNRAS **516,** L1–L6 (2022) https://doi.org/10.1093/mnrasl/slac078
Advance Access publication 2022 July 23

Can we reveal the core-chemical composition of ultra-massive white dwarfs through their magnetic fields?

Maria E. Camisassa,[1]★ Roberto Raddi ,[2] Leandro G. Althaus,[3,4] Jordi Isern,[5,6,7] Alberto Rebassa-Mansergas,[2,6] Santiago Torres,[2,6] Alejandro H. Córsico[3,4] and Lydia Korre[1]

[1]*Department of Applied Mathematics, University of Colorado, Boulder, CO 80309-0526, USA*
[2]*Departament de Física, Universitat Politècnica de Catalunya, c/Esteve Terrades 5, 08860 Castelldefels, Spain*
[3]*Instituto de Astrofísica de La Plata, UNLP-CONICET, Paseo del Bosque s/n, 1900 La Plata, Argentina*
[4]*Facultad de Ciencias Astronómicas y Geofísicas, Universidad Nacional de La Plata, Paseo del Bosque s/n, 1900 La Plata, Argentina*
[5]*Institute of Space Sciences (ICE, CSIC), Campus UAB, Carrer de Can Magrans s/n, 08193 Barcelona, Spain*
[6]*Institut d'Estudis Espacials de Catalunya (IEEC), c/Gran Capità 2-4, Edif. Nexus 201, 08034 Barcelona, Spain*
[7]*Fabra Observatory (RACAB), Rambla dels Estudis 115, 08002 Barcelona, Spain*

Accepted 2022 July 13. Received 2022 July 12; in original form 2022 March 24

ABSTRACT

Ultra-massive white dwarfs ($1.05\,M_{\odot} \lesssim M_{WD}$) are particularly interesting objects that allow us to study extreme astrophysical phenomena such as type Ia supernovae explosions and merger events. Traditionally, ultra-massive white dwarfs are thought to harbour oxygen–neon (ONe) cores. However, recent theoretical studies and new observations suggest that some ultra-massive white dwarfs could harbour carbon–oxygen (CO) cores. Although several studies have attempted to elucidate the core composition of ultra-massive white dwarfs, to date, it has not been possible to distinguish them through their observed properties. Here, we present a new method for revealing the core-chemical composition in ultra-massive white dwarfs that is based on the study of magnetic fields generated by convective mixing induced by the crystallization process. ONe white dwarfs crystallize at higher luminosities than their CO counterparts. Therefore, the study of magnetic ultra-massive white dwarfs in the particular domain where ONe cores have reached the crystallization conditions but CO cores have not, may provide valuable support to their ONe core-chemical composition, since ONe white dwarfs would display signs of magnetic fields and CO would not. We apply our method to eight white dwarfs with magnetic field measurements and we suggest that these stars are candidate ONe white dwarfs.

Key words: stars: interiors – stars: magnetic field – white dwarfs.

1 INTRODUCTION

White dwarf (WD) stars are the most common endpoint of stellar evolution. Therefore, the WD population in our Galaxy is considered a powerful tool to investigate a wide variety of astrophysical problems, from the formation and evolution of our Galaxy to the ultimate fate of planetary systems (see Althaus et al. 2010, for a review). Among all the WD stars, of special interest are those WDs with masses larger than $\sim 1.05\,M_{\odot}$, commonly referred to as 'ultra-massive' WDs. Observations of these stars have been largely reported in the literature (Hollands et al. 2020; Kilic et al. 2021; Caiazzo et al. 2021; Miller et al. 2022), and are considered of special interest as they are related to stellar merger episodes, the occurrence of physical processes in the super asymptotic giant-branch (SAGB) phase, and type Ia Supernovae and micronovae explosions.

Despite the large interest in ultra-massive WDs, there is not a clear consensus on the core-chemical composition of such objects. Traditionally, these stars are thought to be born as a result of the isolated evolution of massive intermediate-mass stars with masses larger than 6–9 $M_{\odot}$, which reach the SAGB with a degenerate core that develops temperatures high enough to ignite carbon. The violent carbon flame propagates through the core, leading to the formation of an ultra-massive WD with a core composed mainly by oxygen (O) and neon (Ne) (Garcia-Berro & Iben 1994; Siess 2010). However, recent theoretical models of the isolated progenitors of ultra-massive WDs suggest that they can avoid carbon burning on the SAGB, leading to the formation of ultra-massive WDs with cores composed mainly by C and O (Althaus et al. 2021). An alternate scenario for the formation of ultra-massive WDs has gained relevance in the last years. It is thought that a relevant fraction of the single massive WDs in our Galaxy have been formed as a result of stellar mergers (Temmink et al. 2020; Cheng et al. 2020; Fleury et al. 2022; Torres et al. 2022). Although this scenario has been explored in several hydrodynamical simulations (Yoon, Podsiadlowski & Rosswog 2007; Lorén-Aguilar, Isern & García-Berro 2009), the core-chemical composition of single ultra-massive WDs born in stellar mergers is a matter of debate. Schwab (2021) simulated the merger of two CO WDs and found that, if the remnant has a mass larger than $\sim 1.05\,M_{\odot}$, then the initial CO core is converted into ONe. On the other hand, Wu, Xiong & Wang (2022) studied the evolution of the remnant of a merger of a massive CO-core WD with a He-core WD and showed that this scenario can lead to the formation of ultra-massive CO-core WDs with masses up to $\sim 1.20\,M_{\odot}$.

★ E-mail: camisassam@gmail.com

Several studies in the literature have tried to distinguish ONe from CO ultra-massive WDs. Hollands et al. (2020) observed a 1.14 $M_{\odot}$ WD with a unique hydrogen/carbon atmosphere composition. These authors tried to use the atmospheric non-detection of O to test the core-chemical composition of this WD. However, despite the distinct core-structures, the outer layers of CO- and ONe-core WDs are almost indistinguishable and therefore the degree of O dredge-up does not depend on the core-composition. A promising avenue to infer the inner chemical stratification of ultra-massive WDs is through Asteroseismology (Córsico et al. 2019a, b, 2021). Nevertheless, in order to pursue such task it is necessary to find a large number of pulsating ultra-massive WDs with abundant detected pulsation periods.

Despite the persisting efforts, the inference of the core composition of ultra-massive WDs has not been possible to date. Here, we present a new method to accomplish this goal, by using the magnetic field measurements in ultra-massive WDs. According to two-component phase diagrams (Medin & Cumming 2010; Horowitz, Schneider & Berry 2010; Blouin et al. 2020) for both CO and ONe mixtures, during the crystallization process, the solid core is enriched in the heavier element (i.e. O in a CO mixture, Ne in an ONe mixture). Therefore, the liquid mantle surrounding the solid core will be depleted in the heavier element, thus having a molecular weight lower than the regions above it and hence inducing a Rayleigh–Taylor mixing in a significant portion of the WD. The pioneering study of Isern et al. (2017) suggested that the compositionally driven convection occurring in these stars could drive dynamo magnetic fields similar to those found in Solar system planets. The studies of Schreiber et al. (2021a), Schreiber et al. (2021b) showed that these crystallization-induced dynamos can generate magnetic fields in cataclysmic variables and in cold metal polluted WDs, explaining their large fraction among the observed population and Belloni et al. (2021) demonstrated that such dynamos can account for the observed rareness of bright intermediate polars in globular clusters. Furthermore, Bagnulo & Landstreet (2021) have analysed the complete volume-limited WD sample within 20 pc from the Sun, showing that the occurrence of magnetic fields is significantly higher in WDs that have fully or partially crystallized cores than in WDs that have not started the crystallization process yet. Here, we propose that crystallization-induced dynamo magnetic fields can be used to infer the core-chemical composition of ultra-massive dwarfs. As previously found in Camisassa et al. (2021), Camisassa et al. (2022) and Bauer et al. (2020), ONe-core WDs crystallize at higher luminosities and effective temperatures than their CO-core counterparts, due to the larger coulomb interactions between their ions. Therefore, we expect a particular region in the colour–magnitude diagram where ONe ultra-massive WDs have started the crystallization process, and hence could be dominated by crystallization-driven dynamos, but CO WDs have not. By analysing eight magnetic WDs in this particular domain, we propose that the presence of magnetic fields in WDs located within that region is evincing their ONe core-chemical composition.

2 THE WHITE DWARF SAMPLE

We selected all known magnetic WDs that are listed in the Montreal White Dwarf Database (Dufour et al. 2017). These stars are shown in the *Gaia* EDR3 colour–magnitude diagram in Fig. 1, together with the hydrogen-rich CO-core and ONe-core WD evolutionary models of Camisassa et al. (2016), Camisassa et al. (2019), Camisassa et al. (2022). We have employed the model atmospheres of Koester (2010) and Koester & Kepler (2019) to convert these evolutionary models

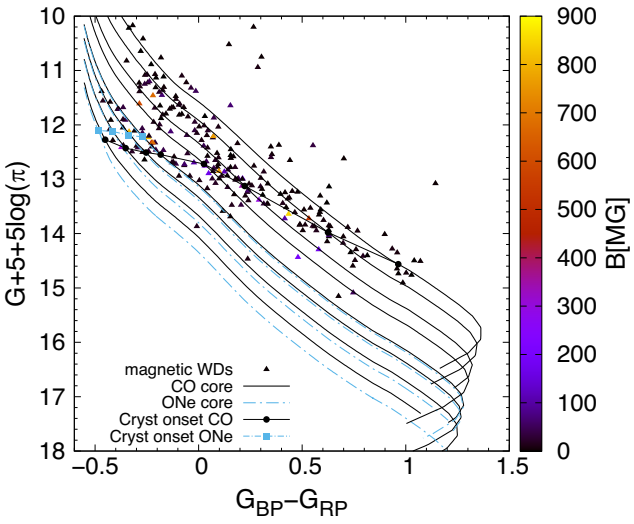

Figure 1. All known magnetic WDs in the *Gaia* EDR3 colour–magnitude diagram taken from the Montreal White Dwarf Database. Colour coding indicates the magnetic field intensity in 10^6 G. The DA CO-core WD evolutionary models with 0.53, 0.66, 0.82, 0.95, 1.10, 1.16, 1.23, and 1.29 $M_{\odot}$ from Camisassa et al. (2016), Camisassa et al. (2022) are indicated using solid black lines. The DA ONe-core WD evolutionary models with 1.10, 1.16, 1.23, and 1.29 $M_{\odot}$ from Camisassa et al. (2019) are displayed using dot–dashed blue lines. The black circles and blue squares indicate the crystallization onset in each sequence, respectively.

into the magnitudes in *Gaia* EDR3 passbands. Crystallization onset in these models is determined by the phase diagrams of Horowitz et al. (2010) and Medin & Cumming (2010) and is shown as black circles and blue squares, respectively. Colour coding indicates the intensity of the magnetic fields (see Ferrario, de Martino & Gänsicke 2015; Ferrario, Wickramasinghe & Kawka 2020, for reviews on magnetic WDs). The magnetic ultra-massive WDs that have larger luminosities than the ONe crystallization onset are not expected to be crystallizing and therefore their magnetic fields must be originated by mechanisms other than crystallization-driven dynamos.

Among all the magnetic WDs, we identified eight objects that lie in the region delimited by the CO and ONe crystallization onset and by the 1.29 and 1.10 $M_{\odot}$ evolutionary sequences. If these ultra-massive WDs harbour an ONe-core, they are undergoing the crystallization process. Otherwise, if they have a CO-core, they have not started this process yet. This set of eight WDs is shown on the *Gaia* colour–magnitude diagram in Fig. 2. All the selected objects are fully within our region of interest, except for SDSS J112030.34−115051.1 that has larger error bars. All of our selected WDs have hydrogen dominated envelopes and only one of them, WD1628+440, has an estimation for its rotation period, which has a lower limit of 6 h and an upper limit of 4 d (Brinkworth et al. 2013). The names and properties of these selected WDs are listed in Table 1.

3 THE WHITE DWARF MODELS

We have employed the ONe-core ultra-massive evolutionary models of Camisassa et al. (2019) to analyse the selected magnetic WDs. These models were calculated using the La Plata stellar evolutionary code LPCODE (see Althaus et al. 2005, 2015, for details). This evolutionary code has been amply used in the study of different aspects of low-mass star evolution (see Camisassa et al. 2016, 2017; Althaus et al. 2021, and references therein). These evolutionary models include a realistic treatment of the crystallization process for

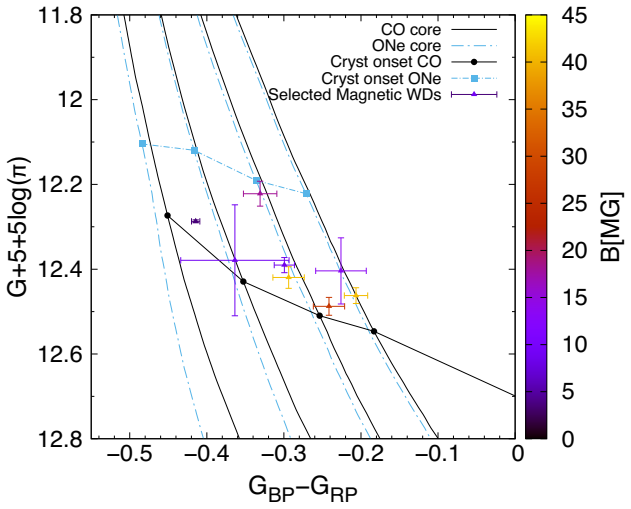

Figure 2. Zoomed-in view of the ONe crystallization region for ultra-massive WDs in the Gaia colour–magnitude diagram. That is, we plot those WDs that, if they harbour ONe cores, they have started the crystallization process, but if they harbour CO cores, they have not. The adopted colours and symbols are the same as in Fig. 1. The error bars account for photometric and parallax uncertainties.

ONe mixtures, using an updated phase diagram (Medin & Cumming 2010), and include the energy released as latent heat and by the phase separation process induced by crystallization. Furthermore, the initial chemical profiles are the result of the full progenitor evolution through the thermally pulsing SAGB, calculated by Siess (2010). These accurate initial chemical profiles play a key role in determining the extension of the Rayleigh–Taylor convective region that will be responsible for generating the dynamos. According to the phase diagram employed, in an ONe WD, the solid core is enriched in Ne and therefore the immediate surrounding liquid layer is depleted in it, leading to a convective region that takes place in a large portion of the star. The extension of this convective region in the 1.16 $M_\odot$ ONe-core model as a function of the logarithm of the stellar luminosity is shown in the top panel of Fig. 3. The inner (outer) boundary of this region is displayed using a dotted blue (solid purple) line. The inner boundary moves outwards as crystallization proceeds, whereas the outer boundary barely moves. These boundaries are determined by the chemical abundances that result from the calculation of the full progenitor evolution.

The bottom panel of Fig. 3 shows the extension of the convective region in the 1.16 $M_\odot$ CO model of Camisassa et al. (2022) as a function of the logarithm of the stellar luminosity. By comparing the top and bottom panels of this figure, we see that for $-2.35 \lesssim \log(L/L_\odot) \lesssim -2$, the 1.16 $M_\odot$ ONe-core model is developing a convective mantle covering up to $\sim$ 88 per cent of its mass, that is absent in the 1.16 $M_\odot$ CO model.

We have interpolated the magnitude G and the colour index G_{BP}–G_{RP} in our ONe-core WD sequences to obtain the values of the mass, the luminosity, the cooling age, the effective temperature, and the logarithm of the surface gravity of the target stars. These quantities are listed in Table 1. For those WDs whose masses are not encompassed in Camisassa et al. (2019), we have specifically calculated evolutionary models, by scaling the initial chemical profile of the most similar model from Camisassa et al. (2019). On the basis of these models, we obtained the fraction of crystallized mass (M_s/M_{WD}) and the thickness of the convective region (r_o–r_i), also listed in Table 1, among other parameters.

4 THE WHITE DWARF DYNAMO

The magnetic Reynolds number and the magnetic Prandtl number are defined as $\mathrm{Rm} = ul/\eta$ and $\mathrm{Pm} = \nu/\eta$, respectively, where u is a typical velocity, l is a typical length, η is the magnetic diffusivity, and ν is the kinematic viscosity. The Ohmic decay time can be estimated as $\tau_\Omega \sim R_{WD}^2/\eta$, where R_{WD} is the WD radius. Isern et al. (2017) estimated that, in a typical massive WD, $\mathrm{Rm} \sim 10^{14}$–10^{15}, $\mathrm{Pm} \sim 0.58$, and τ_Ω is much longer than the WD age. Thus, once the magnetic field has been generated by the convection-driven dynamo, it will be sustained against Ohmic dissipation. In that sense, it is practical to use the dynamo scaling theory of Christensen (2010) to estimate the intensity of the magnetic field in terms of the properties of the convective region, that takes into account the balance between the Ohmic dissipation and the energy flux (in the rapidly rotating regime). Following Christensen (2010) (see also Christensen, Holzwarth & Reiners 2009), we obtain:

$$\frac{B^2}{8\pi} = c f_\Omega \frac{1}{V} \int_{r_i}^{r_o} \left[\frac{q_c(r)\lambda(r)}{H(r)}\right]^{2/3} \rho(r)^{1/3} 4\pi r^2 dr, \quad (1)$$

where the integral is the energy of the convective region (E), B is the magnetic field intensity, c is an adjustable parameter, f_Ω is the ratio between the Ohmic dissipation and the total dissipation, V is the volume of the convective mantle, r_i and r_o are its inner and outer radius, respectively, q_c is the convected energy flux, H is the scale height, and λ is the mixing length. We adopt $f_\Omega = 1$ and $\lambda = H$. The energy density E/V was calculated for each of our selected WDs, and it is listed in Table 1.

This scaling law is applicable for WDs in the rapidly rotating regime, whereby the Rossby number, which is the ratio of inertial force to Coriolis force, is much lower than 1, and the equipartition field strength is achieved. We estimate the Rossby number as $\mathrm{Ro} \sim \frac{P}{t_{conv}}$, where P is the rotation period and t_{conv} is the convective turnover time-scale. We cannot measure the convective turnover time-scale in the WD interior, but we can provide an estimation for it. The density contrast between the floating O enriched material and the surrounding liquid ONe mixture is $\Delta\rho/\rho \sim 10^{-4}$ and therefore its upwards acceleration is $a = g\Delta\rho/\rho \sim 2 \times 10^5\,\mathrm{cm\,s^{-2}}$. Assuming a limiting velocity of the turbulent eddies as in Isern et al. (2017), we obtain a characteristic convective velocity of $3 \times 10^5\,\mathrm{cm\,s^{-1}}$. Therefore, we estimate the convective turnover time-scale for ONe composition to be $\sim$500 s. Measuring the rotation period in WDs is a difficult task. Among the eight WDs analysed in this paper, only WD 1658+440 has a poorly constrained rotation period with an upper limit of 4 d, which suggests that this star is not in a fast-rotating regime.

The dynamo energy density and the measured magnetic field intensity of our selected ultra-massive WDs are plotted in Fig. 4, together with the predictions for the Earth, Jupiter, M dwarfs and T Tauri stars (Christensen et al. 2009), and the WDs studied by Isern et al. (2017). The scaling law of Christensen et al. (2009) considering $c = 0.63$ and a deviation of a factor 3 from it are displayed using solid and dotted black lines, respectively. Five of our eight ultra-massive WDs in our sample match the scaling law within a factor of 10, and the other three match it within a factor of 25. In particular, for WD 1658+440, the agreement between the observed and predicted magnetic field is remarkably good. This generally good agreement suggests that these eight WDs could have ONe cores, since CO-core models would not have reached the crystallization onset and hence

Table 1. Name, spectral type, and magnetic field intensity of our selected ultra-massive WDs, together with our estimations for the mass, luminosity, cooling times, effective temperature, surface gravity, crystallized mass fraction, and length and dynamo energy density of the convective mantle.

Name	Type	B [MG]	M [$M_\odot$]	log ($L/L_\odot$)	t_{cool} [Gyr]	T_{eff} [k]	log g [cgs]	M_s/M_{WD}	r_o–r_i [$\times 10^8$ cm]	E/V [$\times 10^{11}$ erg cm^{-3}]	Ref.
WD 1658+440	DA	3.5	1.243	−1.87	0.291	28763	9.19	0.14	1.47	8.62	(a)
SDSS J205233.51−001610.6	DA	13.42	1.097	−2.36	0.504	18168	8.83	0.19	1.77	1.77	(b)
SDSS J080359.93+122943.9	DA	40.7	1.093	−2.43	0.570	17424	8.83	0.28	1.56	1.43	(b)
SDSS J155708.02+041156.4	DA	41	1.165	−2.20	0.430	21403	8.98	0.20	1.63	2.70	(c)
WD 1131+521	DA	8.64	1.165	−2.17	0.409	21690	8.98	0.16	1.71	2.93	(b)
SDSS J142703.40+372110.5	DA	27.04	1.133	−2.36	0.536	18885	8.91	0.30	1.40	1.97	(b)
WD 1327+594	DQAP	18	1.161	−2.03	0.305	23392	8.96	0.01	2.34	3.68	(d)
SDSS J112030.34−115051.1	DA	8.9	1.22	−2.01	0.359	25383	9.11	0.23	1.41	5.58	(b)

Note. References: (a) Schmidt et al. (1992); (b) Külebi et al. (2009); (c) Kepler et al. (2015); (d) Vanlandingham et al. (2005)

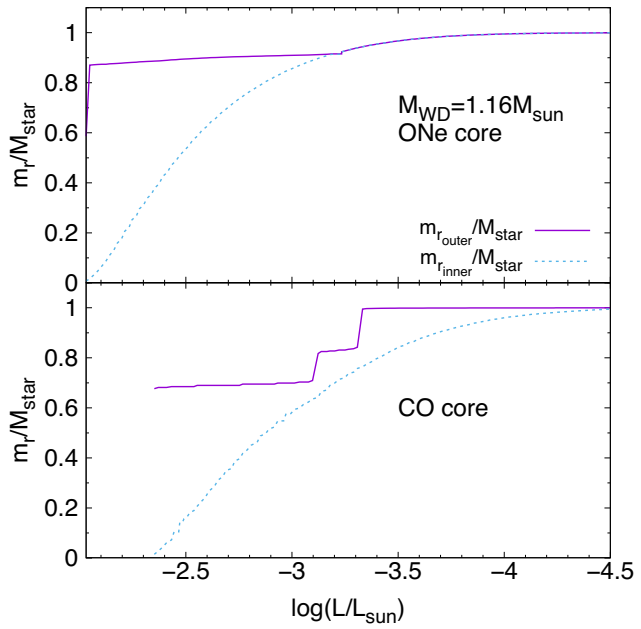

Figure 3. Top panel: Solid purple (dotted blue) line displays the mass fraction at the outer (inner) boundary of the convective region in terms of the logarithm of the stellar luminosity, for our 1.16 $M_\odot$ ONe-core WD model. Bottom panel: Same as top panel, but for our 1.16 $M_\odot$ CO-core WD model.

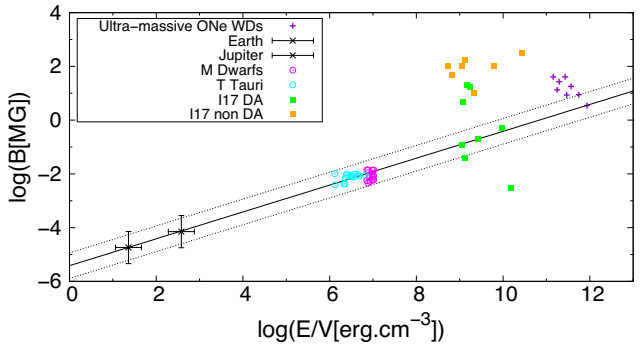

Figure 4. Magnetic field intensity in terms of the dynamo energy density. Earth and Jupiter are indicated using black crosses with error bars, whereas M dwarfs and T Tauri are plotted using magenta and cyan circles, respectively (Christensen et al. 2009). The DA and non-DA WDs from Isern et al. (2017) are shown using green and orange squares, respectively. The ultra-massive WDs listed in Table 1 are plotted using purple crosses. The solid line is the scaling law from Christensen et al. (2009) for the Earth, Jupiter, T Tauri, and M dwarf stars considering $c = 0.63$, and the dotted lines allow for a deviation of a factor of 3 from it.

they would not hold crystallization-driven dynamos. However, we wish to remark that although the agreement we found for our eight ultra-massive WDs is better than the one found in Isern et al. (2017), the observed field distribution of our ONe WD candidates (from ∼3 to ∼40 MG) is not significantly different from the field distribution of all isolated magnetic WDs, since ∼60 per cent of them have field strengths in the range 3–40 MG (see Fig. 11 in Ferrario et al. 2020).

5 SUMMARY AND CONCLUSIONS

Despite the large interest in ultra-massive WDs, there is not a clear consensus in the literature on whether these stars harbour an ONe or a CO core. Aiming at obtaining information on their core-chemical composition, we have analysed a sample of eight magnetic ultra-massive WDs selected from the Montreal White Dwarf Database. These stars lie within a particular domain that implies that, if they harbour an ONe core, they are undergoing the crystallization process, whereas if they harbour a CO core, they have not started this process yet. That is, ONe core WDs in this region should have a convective region that drives dynamo magnetic fields, but CO WDs should not. Relying on precise ONe ultra-massive WD evolutionary models from Camisassa et al. (2019) that include realistic chemical profiles that result from the full progenitor evolution, and an updated treatment of the chemical redistribution induced by crystallization, we have modelled these candidate ONe WDs. We have estimated their mass, their luminosity, their percentage of crystallized mass, the length of their convective mantles, and their convective energy density, among other parameters.

We have compared the measured magnetic fields of these stars with the estimations of the dynamos predicted by the scaling law of Christensen et al. (2009), which is suitable for the Earth, Jupiter, M dwarfs, and T Tauri stars in the rapidly rotating regime. Among our sample of eight WDs, only WD 1658+440 has a poorly constrained measurement of the rotating period, with an upper limit of 4 d. Therefore, we cannot predict whether these eight WDs are in the rapidly rotating regime. The magnetic field measurements of WD 1658+440, SDSS J205233.51-001610.6, WD 1131+521, WD 1327+594, and SDSS J112030.34−115051.1 match the magnetic field intensity predicted by the scaling law within a factor of 10, indicating that they will likely harbour ONe cores. In particular, the agreement between the predicted and observed magnetic field for WD 1658+440 is remarkably good, evincing its ONe core. The magnetic field measurements for SDSS J080359.93+122943.9, SDSS J155708.02+041156.4, and SDSS J142703.40+372110.5 exceed the scaling law by a factor of ∼20. The high magnetic fields in these WDs could be indicating that these stars are very fast rotators. Recent numerical simulations suggest that fast rotating

convective dynamos with Ro $\ll 1$ can achieve super-equipartition magnetic fields (Augustson, Brun & Toomre 2016, 2019). In that context, Ginzburg et al. (2022) claimed that the density contrast driving the convective zone could be smaller than the one used in this paper and in Mochkovitch (1983) and Isern et al. (2017), yielding convective turnover time-scales longer than those used here, opening the possibility to these white dwarf to be fast rotators with strong magnetic fields. Furthermore, the scaling law that we use has been determined for planets, M dwarfs, and T-Tauri stars, where the magnetic Prandtl number is 5–6 orders of magnitudes smaller than in WDs. Considering a likely dependence of the dynamo efficiency on the magnetic Prandtl number, we could expect that the WD dynamo can generate magnetic fields larger than the predictions of the scaling law (see Schreiber et al. 2021a, for a thorough discussion), implying that SDSS J080359.93+122943.9, SDSS J155708.02+041156.4, and SDSS J142703.40+372110.5 can also have an ONe core.

Finally, we cannot disregard that the magnetic fields in these WDs could be fossil fields (Braithwaite & Spruit 2004), generated during the merger of two WDs (García-Berro et al. 2012) or in a common envelope phase, if the binary companion has been destroyed or is in a wide orbit (Tout et al. 2008). However, none of these scenarios can account for the number of observed magnetic cataclysmic variables, intermediate polar WDs in globular clusters, and cold metal polluted WDs (Schreiber et al. 2021a; Belloni et al. 2021; Schreiber et al. 2021b), implying that the crystallization-induced dynamos must take place. Furthermore, the analysis of the complete volume-limited WD sample within 20 pc from the Sun (Bagnulo & Landstreet 2021) has shown that the occurrence of magnetic fields is significantly higher in WDs that have fully or partially crystallized cores than in WDs with fully liquid cores. In this study, magnetic WDs account for 20 per cent of the sample and the presence of magnetic fields in WDs with fully liquid cores is $\sim$11 per cent, whereas this percentage raises to $\sim$30 per cent for WDs that are undergoing or have undergone the crystallization process. This trend is indicating that the crystallization process could be one important cause for developing magnetic fields in WDs. Due to the absence of ultra-massive WDs within the 20-pc sample, such a population analysis should be extended to a larger volume in the Solar neighbourhood. However, the spectral characterization of the volume-complete 100 pc is still scarce. Within 100 pc from the Sun, the frequency of the occurrence of magnetic fields in ultra-massive WDs with fully liquid cores is $\sim$21 per cent, whereas this frequency decreases to 3 per cent for WDs with partially or fully crystallized cores. This drop does not imply that magnetic fields are more frequent in bright young WDs, but it is the likely consequence of various observational biases. Because the main methods for detecting and measuring magnetic fields take advantage of the Zeeman effect that splits the spectral lines and polarizes them, high signal-to-noise ratio as well as high spectral resolution are needed for the analysis of both weak ($<$1–2 MG) and very strong ($\gtrsim$100 MG) magnetic fields (Landstreet & Bagnulo 2019; Bagnulo & Landstreet 2021). Both requirements, combined to the only recent making of the *Gaia* 100-pc sample (Jiménez-Esteban et al. 2018), have worked against the completeness of an intrinsically fainter sample of ultra-massive magnetic WDs. By extrapolating the population analysis of magnetic WDs within 20-pc to the larger volume, we estimate that there should be nearly 2700 magnetic WDs within 100 pc, but just 125 of them are known so far. An exhaustive search for magnetic fields in all ultra-massive WDs within 100 pc would be needed to fully confirm our results.

Finally, the fact that some WDs that lie in our region of interest have no detected magnetic fields does not imply that these WDs have a CO core, since these WDs could have ONe cores and be crystallizing, but their dynamos are not efficient enough to generate observable magnetic fields. We suggest that, in order to elucidate the core-chemical composition of ultra-massive WDs, efforts should be placed in measuring magnetic fields for large samples of such stars. We expect that close-to-complete large samples of magnetic WDs will be achieved in the next 5–10 yr, thanks to the ongoing and currently developing multi-fibre spectroscopic surveys such as DESI (DESI Collaboration et al. 2016), SDSS-V (Kollmeier et al. 2017), WEAVE (Dalton et al. 2012), and 4MOST (de Jong et al. 2012).

ACKNOWLEDGEMENTS

This work was supported by the NASA grants 80NSSC17K0008, 80NSSC20K0193, and 80NSSC21K0455, the postdoctoral fellowship programme Beatriu de Pinós agreement no. 801370, by AGENCIA through the Programa de Modernización Tecnológica BID 1728/OC-AR, by the PIP 112200801-00940 grant from CONICET, by grant G149 from National University of La Plata, by the MINECO grant PID2020-117252GB-I00, by the ESP 2017-82674-R, by grant RYC-2016-20254 funded by MCIN/AEI/10.13039/501100011033 and by ESF Investing in your future. This work has made use of data from the European Space Agency (ESA) mission *Gaia*, processed by the *Gaia* Data Processing and Analysis Consortium.

DATA AVAILABILITY

Supplementary material will be shared on request to the corresponding author.

REFERENCES

Althaus L. G. et al., 2021, A&A, 646, A30
Althaus L. G., Camisassa M. E., Miller Bertolami M. M., Córsico A. H., García-Berro E., 2015, A&A, 576, A9
Althaus L. G., Córsico A. H., Isern J., García-Berro E., 2010, A&A Rev., 18, 471
Althaus L. G., Serenelli A. M., Panei J. A., Córsico A. H., García-Berro E., Scóccola C. G., 2005, A&A, 435, 631
Augustson K. C., Brun A. S., Toomre J., 2016, ApJ, 829, 92
Augustson K. C., Brun A. S., Toomre J., 2019, ApJ, 876, 83
Bagnulo S., Landstreet J. D., 2021, MNRAS, 507, 5902
Bauer E. B., Schwab J., Bildsten L., Cheng S., 2020, ApJ, 902, 93
Belloni D., Schreiber M. R., Salaris M., Maccarone T. J., Zorotovic M., 2021, MNRAS, 505, L74
Blouin S., Daligault J., Saumon D., Bédard A., Brassard P., 2020, A&A, 640, L11
Braithwaite J., Spruit H. C., 2004, Nature, 431, 819
Brinkworth C. S., Burleigh M. R., Lawrie K., Marsh T. R., Knigge C., 2013, ApJ, 773, 47
Caiazzo I. et al., 2021, Nature, 595, 39
Camisassa M. E. et al., 2019, A&A, 625, A87
Camisassa M. E., Althaus L. G., Córsico A. H., Vinyoles N., Serenelli A. M., Isern J., Miller Bertolami M. M., García-Berro E., 2016, ApJ, 823, 158
Camisassa M. E., Althaus L. G., Koester D., Torres S., Pons P. G., Córsico A. H., 2022, MNRAS, 511, 5198
Camisassa M. E., Althaus L. G., Rohrmann R. D., García-Berro E., Torres S., Córsico A. H., Wachlin F. C., 2017, ApJ, 839, 11
Camisassa M. E., Althaus L. G., Torres S., Córsico A. H., Rebassa-Mansergas A., Tremblay P.-E., Cheng S., Raddi R., 2021, A&A, 649, L7
Cheng S., Cummings J. D., Ménard B., Toonen S., 2020, ApJ, 891, 160
Christensen U. R., 2010, Space Sci. Rev., 152, 565
Christensen U. R., Holzwarth V., Reiners A., 2009, Nature, 457, 167
Córsico A. H., Althaus L. G., Gil Pons P., Torres S., 2021, A&A, 646, A60
Córsico A. H., Althaus L. G., Miller Bertolami M. M., Kepler S. O., 2019a, A&A Rev., 27, 7

Córsico A. H., De Gerónimo F. C., Camisassa M. E., Althaus L. G., 2019b, A&A, 632, A119
Dalton G. et al., 2012, in McLean I. S., Ramsay S. K., Takami H., eds, Proc. SPIE Conf. Ser. Vol. 8446, Ground-based and Airborne Instrumentation for Astronomy IV. SPIE, Bellingham, p 12
de Jong R. S. et al., 2012, in McLean I. S., Ramsay S. K., Takami H., eds, Proc. SPIE Conf. Ser. Vol. 8446, Ground-based and Airborne Instrumentation for Astronomy IV. SPIE, Bellingham, p 15
DESI Collaboration et al., 2016, preprint (arXiv:1611.00036)
Dufour P., Blouin S., Coutu S., Fortin-Archambault M., Thibeault C., Bergeron P., Fontaine G., 2017, in Tremblay P. E., Gaensicke B., Marsh T., eds, ASP Conf. Ser. Vol. 509, 20th European White Dwarf Workshop. Astron. Soc. Pac., San Francisco, p. 3
Ferrario L., de Martino D., Gänsicke B. T., 2015, Space Sci. Rev., 191, 111
Ferrario L., Wickramasinghe D., Kawka A., 2020, Adv. Space Res., 66, 1025
Fleury L., Caiazzo I., Heyl J., 2022, MNRAS, 511, 5984
García-Berro E. et al., 2012, ApJ, 749, 25
Garcia-Berro E., Iben I., 1994, ApJ, 434, 306
Ginzburg S., Fuller J., Kawka A., Caiazzo I., 2022, MNRAS, 514, 4111
Hollands M. A. et al., 2020, Nat. Astron., 4, 663
Horowitz C. J., Schneider A. S., Berry D. K., 2010, Phys. Rev. Lett., 104, 231101
Isern J., García-Berro E., Külebi B., Lorén-Aguilar P., 2017, ApJ, 836, L28
Jiménez-Esteban F. M., Torres S., Rebassa-Mansergas A., Skorobogatov G., Solano E., Cantero C., Rodrigo C., 2018, MNRAS, 480, 4505
Kepler S. O. et al., 2015, MNRAS, 446, 4078
Kilic M., Bergeron P., Blouin S., Bédard A., 2021, MNRAS, 503, 5397
Koester D., 2010, Mem. Soc. Astron. Italiana, 81, 921
Koester D., Kepler S. O., 2019, A&A, 628, A102
Kollmeier J. A. et al., 2017, preprint (arXiv:1711.03234)
Külebi B., Jordan S., Euchner F., Gänsicke B. T., Hirsch H., 2009, A&A, 506, 1341
Landstreet J. D., Bagnulo S., 2019, A&A, 623, A46
Lorén-Aguilar P., Isern J., García-Berro E., 2009, A&A, 500, 1193
Medin Z., Cumming A., 2010, Phys. Rev. E, 81, 036107
Miller D. R., Caiazzo I., Heyl J., Richer H. B., Tremblay P.-E., 2022, ApJ, 926, L24
Mochkovitch R., 1983, A&A, 122, 212
Schmidt G. D., Bergeron P., Liebert J., Saffer R. A., 1992, ApJ, 394, 603
Schreiber M. R., Belloni D., Gänsicke B. T., Parsons S. G., 2021b, MNRAS, 506, L29
Schreiber M. R., Belloni D., Gänsicke B. T., Parsons S. G., Zorotovic M., 2021a, Nat. Astron., 5, 648
Schwab J., 2021, ApJ, 906, 53
Siess L., 2010, A&A, 512, A10
Temmink K. D., Toonen S., Zapartas E., Justham S., Gänsicke B. T., 2020, A&A, 636, A31
Torres S., Canals P., Jiménez-Esteban F. M., Rebassa-Mansergas A., Solano E., 2022, MNRAS, 511, 5462
Tout C. A., Wickramasinghe D. T., Liebert J., Ferrario L., Pringle J. E., 2008, MNRAS, 387, 897
Vanlandingham K. M. et al., 2005, AJ, 130, 734
Wu C., Xiong H., Wang X., 2022, MNRAS, 512, 2972
Yoon S. C., Podsiadlowski P., Rosswog S., 2007, MNRAS, 380, 933

This paper has been typeset from a TEX/LATEX file prepared by the author.